

Correlation of Local Effects of DNA Sequence and Position of β -Alanine Inserts with Polyamide–DNA Complex Binding Affinities and Kinetics

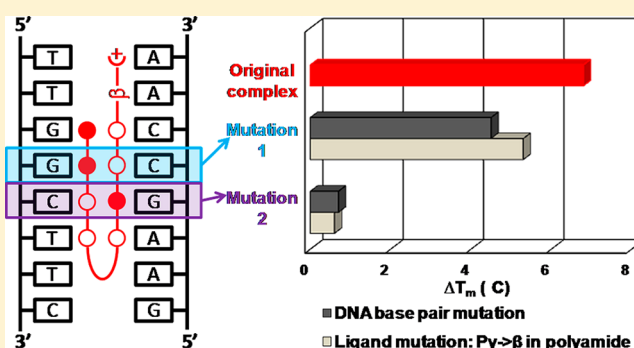
Shuo Wang,[†] Rupesh Nanjunda,[†] Karl Aston,[‡] James K. Bashkin,^{*,‡} and W. David Wilson^{*,†}

[†]Department of Chemistry, Georgia State University, Atlanta, Georgia 30303, United States

[‡]Department of Chemistry and Biochemistry, Center for Nanoscience, University of Missouri—St. Louis, St. Louis, Missouri 63121, United States

S Supporting Information

ABSTRACT: To improve our understanding of the effects of β -alanine (β) substitution and the number of heterocycles on DNA binding affinity and selectivity, we investigated the interactions of an eight-ring hairpin polyamide (PA) and two β derivatives as well as a six-heterocycle analogue with their cognate DNA sequence, 5'-TGGCTT-3'. Binding selectivity and the effects of β have been investigated with the cognate and five mutant DNAs. A set of powerful and complementary methods have been employed for both energetic and structural evaluations: UV melting, biosensor surface plasmon resonance, isothermal titration calorimetry, circular dichroism, and a DNA ligation ladder global structure assay. The reduced number of heterocycles in the six-ring PA weakens the binding affinity; however, the smaller PA aggregates significantly less than the larger PAs and allows us to obtain the binding thermodynamics. The PA–DNA binding enthalpy is large and negative with a large negative ΔC_p and is the primary driving component of the Gibbs free energy. The complete SPR binding results clearly show that β substitutions can substantially weaken the binding affinity of hairpin PAs in a position-dependent manner. More importantly, the changes in the binding of PA to the mutant DNAs further confirm the position-dependent effects on the PA–DNA interaction affinity. Comparison of mutant DNA sequences also shows a different effect in recognition of T·A versus A·T base pairs. The effects of DNA mutations on binding of a single PA as well as the effects of the position of β substitution on binding tell a clear and very important story about sequence-dependent binding of PAs to DNA.



Polyamides (PAs) have been developed from AT-specific-binding natural products into a broad, sequence-specific class of minor groove binding agents.^{1–4} These compounds have had a significant impact on our understanding of DNA molecular recognition, transcription factor binding and inhibition, and DNA allosteric transitions.^{5–7} In a very exciting step forward in the development of these compounds, several groups have shown that they can be taken up by cells in significant amounts and in reasonable time periods. These cellular observations have led to the expanded development of therapeutic applications for PAs, and animal testing has been initiated.^{8–13}

Although PAs have been the subject of extensive development for DNA minor groove binding, they are complicated agents, and more detailed information about the effects of DNA and PA sequence on their interaction energetics is needed for a complete understanding. In therapeutic development of PAs, it is generally useful to incorporate a β in place of one or more heterocyclic units, for example, to allow the compounds to better conform to the shape of the DNA minor groove.^{8,14–16} In a search for compounds to inhibit binding of the transcription factor to the human COX2 promoter, a striking decrease in binding affinity

was observed for a β -substituted PA.¹⁷ Because of a major development of PAs in targeting for elimination the circular genomic DNA molecules of high-risk human papillomavirus (HPV) from human keratinocyte cell and tissue cultures and the observation that antiviral efficacy varies dramatically for positional isomers in which β and *N*-methylpyrrole building blocks are swapped,⁸ it is essential to improve our understanding of the positional effects of heterocyclic substitution by β to design the optimal DNA targeting drugs. To help define the basis for the unexpected energetic cost of β substitution, we present more detailed studies of several PA–DNA complexes. An unfavorable β substitution effect was originally observed in an eight-ring hairpin PA with the β substitution on the *N*-terminal side of the γ hairpin loop [KA1007 (Figure 1)].¹⁷ An additional compound of the same heterocycle composition, but with the β substitution on the *C*-terminal side of the loop (KA1055), has now been

Received: September 28, 2012

Revised: November 19, 2012

Published: November 20, 2012



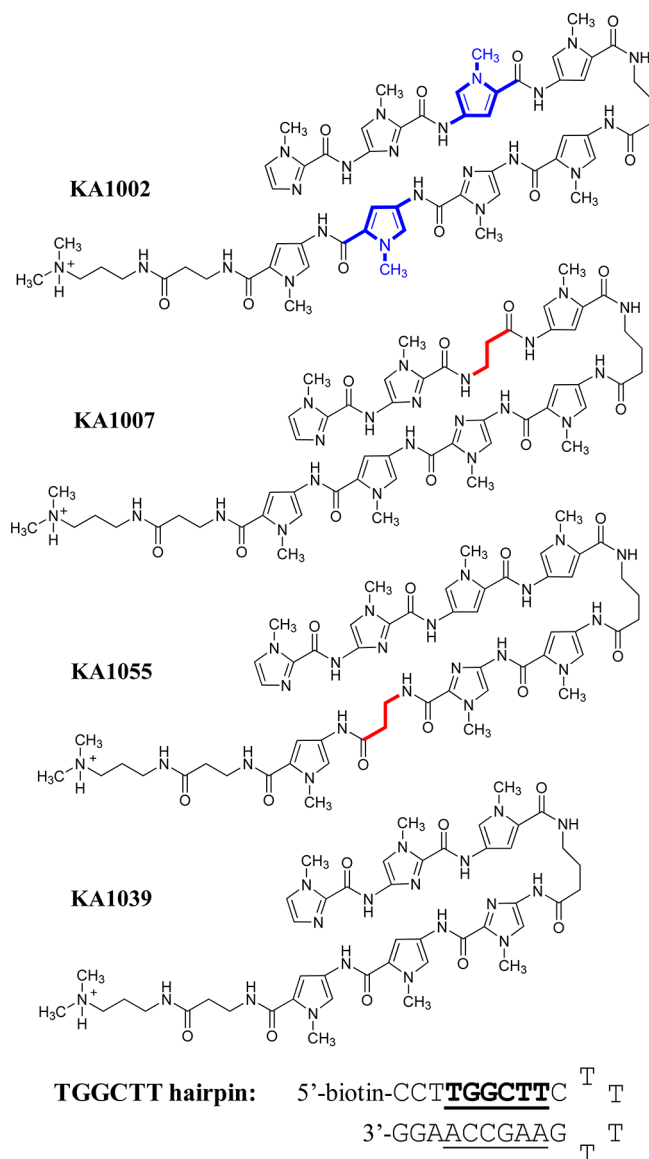


Figure 1. Polyamide structures and their cognate DNA sequence. Note that KA1002 has eight heterocyclic rings, KA1007 and KA1055 have seven rings with one β linker, and KA1039 has six heterocyclic rings. All four polyamides target the TGGCTT DNA sequence (see Table 1).

synthesized to evaluate positional effects of substitution relative to the loop. To determine the energetic effects of simply removing heterocycles from the eight-ring PA, a six-ring PA (KA1039) that binds to the same DNA sequence has also been synthesized and evaluated. Five DNA sequences with one or two base pair mutations in different positions have been studied to evaluate the positional role of DNA base pairs in the PA–DNA complexes. A powerful and complementary set of energetic and structural methods have been used here to study the PA–DNA interactions: thermal melting (T_m), biosensor surface plasmon resonance (SPR), isothermal titration calorimetry (ITC), circular dichroism (CD), and DNA ligation ladder polyacrylamide gel electrophoresis (PAGE). The results show a large effect of the β substitution placement, the DNA base mutation position, and the number of heterocyclic rings on PA–DNA interaction and DNA structure.

MATERIALS AND METHODS



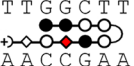

Polyamides, DNAs, and Buffers. All the PAs in this study were synthesized previously¹⁸ except for KA1055 (Figures S1–S9 of the Supporting Information). KA1055 was purified twice by reverse phase high-performance liquid chromatography (HPLC): the first case resulted in nonstoichiometric ammonium trifluoroacetate ($[\text{NH}_4]^+$ was observed in the ^1H NMR) derived from trace ammonia present in Aldrich HPLC-grade MeOH; the second case used ammonia-free mobile phase and gave the expected $(\text{TFA})_3$ salt with no extra ammonium ion. ^1H NMR at 500 and 600 MHz (in $\text{DMSO}-d_6$ with and without a drop of D_2O), elemental analysis (for C, H, N, and F), and HPLC–MS data are provided in the Supporting Information. High-resolution mass spectrometry (HRMS) was also conducted to help prove the identity of KA1055: HRMS (MS^n ESI $^+$) calcd for $\text{C}_{54}\text{H}_{70}\text{N}_{21}\text{O}_{10}$ MH^+ 1172.56145, found 1172.55845. DNA oligomers were purchased from Integrated DNA Technologies, Inc. (IDT, Coralville, IA), with HPLC purification and mass spectrometry characterization. 5'-Biotin-labeled hairpin DNA TGGCTT [5'-biotin-CCTTGGCTTCTTTGAAGCCAA-GG-3' (Figure 1)] with the hairpin loop sequence underlined was used in surface plasma resonance experiments. The same sequence without biotin was used for thermal melting, isothermal titration calorimetry, and circular dichroism experiments. A 21 bp duplex with two phased TGGCTT motifs was used as the ligation ladder in polyacrylamide gel electrophoresis.

HEPES buffer containing 10 mM HEPES, 50 mM NaCl, and 1 mM EDTA (pH 7.4) was used for UV melting, ITC, and CD experiments. The SPR experiments were performed in filtered, degassed HEPES buffer with 0.05% (v/v) surfactant P20. TBE buffer contained 89 mM Tris, 89 mM boric acid, and 2 mM EDTA (pH 8.3) and was used for the gel electrophoresis experiment.

Biosensor Surface Plasmon Resonance. SPR measurements were performed with four-channel Biacore T200 and T100 optical biosensor systems (GE Healthcare, Inc., Piscataway, NJ) at 25 °C. A streptavidin-derivatized (SA) sensor chip was prepared for use by conditioning with a series of 60 s injections of 1 M NaCl in 50 mM NaOH (activation buffer) followed by extensive washing with HBS buffer [10 mM HEPES, 150 mM NaCl, 3 mM EDTA, and 0.05% P20 (pH 7.4)]. Biotinylated DNA samples (25–50 nM) were prepared in HBS buffer and immobilized on the flow cell surface by noncovalent capture as previously described.¹⁹ Flow cell 1 was left blank as a reference, while flow cells 2–4 were immobilized with DNA by manual injection of DNA stock solutions (flow rate of 1 $\mu\text{L}/\text{min}$) until the desired amount of DNA response units (RU) was obtained (350–400 RU). Ligand solutions were prepared with degassed and filtered HEPES buffer by serial dilutions from a concentrated stock solution. Typically, a series of different ligand concentrations (from 1 nM to 1 μM) were injected over the DNA sensor chip at a flow rate of 25 $\mu\text{L}/\text{min}$ until a constant steady-state response was obtained (5–10 min), and this was followed by buffer flow for ligand dissociation (10–15 min). After each cycle, the sensor chip surface was regenerated with a 10 mM glycine solution at pH 2.5 for 30 s followed by multiple buffer injections to yield a stable baseline for the following cycles.

Steady-state equilibrium binding analyses were performed by linear averaging of the observed response (RU_{obs}) in the steady-state region over a selected time region at different compound concentrations and converting them to the moles of bound ligand per mole of DNA, $\text{RU}_{\text{obs}}/\text{RU}_{\text{max}}$, where RU_{max} is the

Table 1. T_m Analyses, Kinetic Rate Constants, and Equilibrium Affinities for the Different Hairpin PAs with Their Cognate DNA Sequence*

	KA1002	KA1007	KA1055	KA1039
				
$\Delta T_m \pm 0.5^\circ\text{C}$	6.8	0.6	5.3	3.2
$k_a (\times 10^6 \text{ M}^{-1} \text{ s}^{-1})$	44 ± 15	5 ± 2	5 ± 2	3 ± 1.5
$k_d (\times 10^{-3} \text{ s}^{-1})$	12 ± 2	170 ± 10	6 ± 1	21 ± 5
$K_A (\times 10^8 \text{ M}^{-1})$	37 ± 7	0.29 ± 0.01 $0.27 \pm 0.02^{\S}$	12 ± 2	1.4 ± 0.2
$K_D (\text{nM})$	0.3 ± 0.1	35 ± 3	0.9 ± 0.2	7.1 ± 0.7

*The errors in these values are based on experimental reproducibility. [§]Only for KA1007 could the K_A value be determined by both kinetic (top) and steady-state (bottom) fitting using a single-site binding model (Materials and Methods).

predicted maximal response per bound compound and was calculated from the DNA molecular weight, the compound molecular weight, the amount of DNA immobilized on the flow cell, and the refractive index gradient ratio of the compound and DNA, as previously described.²⁰ RU_{obs} was plotted as a function of free ligand concentration (C_{free}), and the equilibrium binding constants (K_A) were determined with a one-site binding model using nonlinear least-squares optimization to obtain an optimal fit for RU_{obs} using $RU_{\text{max}} \times (K_A C_{\text{free}}) / (1 + K_A C_{\text{free}})$. RU_{max} in the equation was used as a fitting parameter, and the obtained value was compared to the predicted maximal response per bound ligand to independently evaluate the stoichiometry.²⁰ Kinetic analysis was performed by globally fitting the binding results for the entire concentration series using a standard 1:1 kinetic model with integrated mass transport-limited binding parameters as described previously.^{21,22}

Isothermal Titration Calorimetry. ITC experiments were performed using a MicroCal VP-ITC (MicroCal Inc., Northampton, MA) interfaced with a computer equipped with VP-2000 software for instrument control and Origin 7.0 for data analysis. The sample cell was filled with 10 μM hairpin DNA in HEPES buffer, and 30 injections of 10 μL of the compound solution were performed incrementally. A delay of 300 s was used between each injection to ensure the equilibration of the baseline. The heat for each injection was obtained by integration of the peak area as a function of time. The heats of dilution, determined by injecting the compound into the sample cell containing only buffer, were subtracted from those in compound/DNA titrations to present the corrected binding-induced enthalpy changes. A range of compound concentrations and temperatures were used in these experiments to optimize conditions for data collection.

UV Thermal Melting. DNA melting (T_m) curves were recorded with a Cary 300 UV–visible spectrophotometer (Varian Inc., Palo Alto, CA) equipped with a thermoelectrically controlled cell holder. The absorbances of the free DNA and PA–DNA complex were measured at 260 nm in 1 cm quartz cuvettes from 25 to 95 $^\circ\text{C}$ with a heating rate of 0.5 $^\circ\text{C}/\text{min}$. The DNA concentration was 3 μM in hairpin, while the concentrations of PAs ranged from 0 to 6 μM . The T_m curves were normalized to give equimolar DNA concentrations. All the thermal melting experiments were conducted three times.

Circular Dichroism. CD spectra were recorded using a Jasco J-810 spectrometer (Jasco Inc., Easton, MD) from 450 to 230 nm with 1 cm quartz cuvettes at 25 $^\circ\text{C}$. The spectra were averaged over four scans with a scan speed of 50 nm/min and a buffer

blank correction. A 5 μM DNA solution was first scanned; the compounds at increasing concentration ratios were then titrated into the same cuvette, and the complexes were scanned under the same conditions.

Ligation Ladders and Gel Electrophoresis. A 21-base single-strand DNA with two phased TGGCTT sites and its complementary strand were combined in a 1:1 molar ratio and annealed in 1 \times ligation buffer (New England Biolabs, Ipswich, MA) containing 50 mM Tris-HCl, 10 mM MgCl_2 , 10 mM dithiothreitol, and 1 mM ATP. Annealed duplexes were 5'-phosphorylated using T4 polynucleotide kinase (New England Biolabs) for 30 min at 37 $^\circ\text{C}$ followed by enzyme deactivation at 65 $^\circ\text{C}$ for 20 min. These duplexes were then ligated with T4 DNA ligase (New England Biolabs) at room temperature for 20 min followed by an inactivation time of 20 min at 65 $^\circ\text{C}$. M21, a 21-mer sequence used as the mobility standard, and A5, which is the reference sequence for curvature calculation, were annealed and ligated in the same procedure. For an additional set of markers varying in length by 20 bp (Bayou Biolabs, Metairie, LA), a commercially available standard sequence with the 100 bp band at double intensity was used.

Ligation ladders were separated on an 8% native polyacrylamide gel (1.5 mm thick, 20 cm long) prepared from a 40% acrylamide solution [29:1 acrylamide:bisacrylamide ratio (EMD, Gibbstown, NJ)] in 1 \times TBE buffer. Electrophoresis was conducted at 200 V (10 V/cm) and 25 $^\circ\text{C}$ for 170 min in a Bio-Rad Protean II xi gel apparatus using a Bio-Rad PowerPac Basic 300. Each sample contained 2 μM ligation ladders and compounds at a 4:1 concentration ratio of ligand to TGGCTT site. After electrophoresis, gels were stained with SYBR Gold Nucleic Acid Gel Stain (Invitrogen, Carlsbad, CA) at the concentration recommended by the manufacturer for 1 h. The stained gels were imaged using an UltraLum Omega 10gD Molecular Imaging System (UltraLum, Claremont, CA). Migration analysis and molecular weight assignment were performed with Image Quant TL (GE Healthcare, Inc.).

RESULTS

Thermal Melting: Qualitative Comparison of Binding Affinity. Thermal melting is a rapid and qualitative method for comparison of relative compound binding affinities for DNA.²³ PA screening experiments by thermal melting were conducted with the TGGCTT target sequence and the PAs of Figure 1. The ΔT_m value, the T_m of the complex minus the T_m of free DNA, for each PA at 1:1 compound:DNA molar ratio allows the binding

affinities to be ranked. Melting curves are compared in Figure S10 of the Supporting Information, and ΔT_m values are listed in Table 1. KA1002 increased the T_m of DNA the most, 6.8 °C, while the ΔT_m values for KA1007, KA1055, and KA1039 were 0.6, 5.3, and 3.2 °C, respectively, with an error of ± 0.5 °C.

The binding affinities of KA1002 and KA1055 with five mutant DNA sequences (Figure S11 of the Supporting Information) were evaluated by thermal melting at a 1:1 molar ratio, and the results are listed in Table 2. The thermal stability of the

Table 2. T_m Analyses for KA1002 and KA1055 with TGGCTT and Five Mutant Sequences

	DNA sequence	T_m (°C) for free DNA	ΔT_m^a (°C) for KA1002	ΔT_m^a (°C) for KA1055
	TGGCTT	74.0	6.8	5.3
mutant 1	TGCCTT	74.1	11.3	6.2
mutant 2	TGTCTT	68.2	4.5	3.4
mutant 3	TGGGTT	73.5	0.7	0.6
mutant 4	TGGCCT	78.8	3.1	1.3
mutant 5	TGATTT	65.6	0.5	0.8

^aThe error of these ΔT_m values is ± 0.5 °C, based on experimental reproducibility.

TGGCTT mutant sequence was enhanced by the PAs compared to that of the original TGGCTT site, while the ΔT_m values for the other mutant sites are all smaller than for TGGCTT. Because TGGCTT has a cognate binding site for KA1002 and KA1055, while the other mutant DNAs do not, the reduced ΔT_m values

are as expected, but the sequence dependence of the effects is large. The sequence effects are discussed in detail below.

Surface Plasmon Resonance: Quantitative Determination of Binding Affinity and Kinetics. Biosensor SPR provides a sensitive technique for monitoring the progress of reactions in real time to yield the kinetics as well as the equilibrium binding affinities of biomolecular interactions.¹⁹ To quantitatively evaluate the binding interactions of the hairpin PAs with their target DNA sequence and also to provide details about the positional effects of the substitution of Py by the internal β , SPR experiments were conducted with a hairpin duplex containing the cognate binding site, 5'-TGGCTT-3' (Figure 2). It is clear from the shape of the binding curves that different PAs have varying on and off rates with the DNA with a strong effect of β substitution. The rate constants obtained from global kinetic fitting of the sensorgrams and the equilibrium binding constants for the different PAs are listed in Table 1.

KA1002, the parent PA without β substitutions, clearly stands out as the strongest binder with the cognate sequence [$K_A = (37 \pm 7) \times 10^8 \text{ M}^{-1}$ (Table 1)]. The strong binding observed with this compound can be attributed to the fast association and the very slow dissociation rates (Table 1). The single substitution of one of the pyrrole moieties with a β on the N-terminal side of the KA1002 hairpin loop results in a dramatic 120-fold decrease in the binding affinity of KA1007 with the cognate sequence [$K_A = (0.29 \pm 0.01) \times 10^8 \text{ M}^{-1}$]. This β substitution decreases the association rate of the ligand by a factor of 10 (Table 1) when compared to that of KA1002, but much of the decrease in the

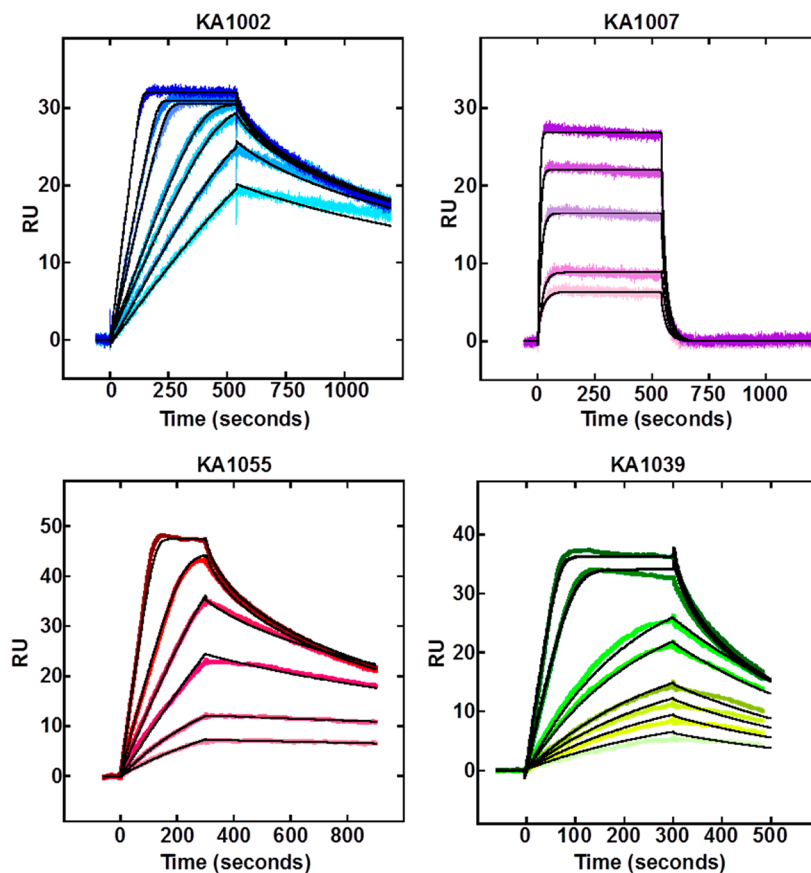


Figure 2. SPR sensorgrams (color) and global kinetic fits (black overlays) for all PAs with the cognate TGGCTT DNA sequence. The concentrations from bottom to top are 1.5, 2, 2.5, 3, 5, 6, and 9 nM for KA1002; 5, 10, 20, 40, and 60 nM for KA1007; 2, 3, 4, 6, 8, and 15 nM for KA1055; and 2, 3, 4, 5, 8, 10, 20, and 30 nM for KA1039.

binding affinity observed is a consequence of the faster rate of dissociation of KA1007 from DNA (~ 15 -fold larger k_d than for KA1002). The faster dissociation of KA1007 is evident in the sensorgrams (Figure 2) where much of the compound has dissociated from DNA within the first few seconds of the dissociation phase.

Interestingly, a similar β substitution of a pyrrole unit on the C-terminal side of the γ hairpin loop (KA1055) results in an only 3-fold decrease in the binding affinity relative to that of KA1002. Although the association rate constant of KA1055 is 10-fold lower than that for KA1002, the binding affinity is only 3-fold lower because of a dissociation rate for KA1055 that is 2-fold slower than that for KA1002. It should be noted that even though the association rates of the two PAs with a single β substitution (KA1007 vs KA1055) are very similar, the dissociation rates differ by a factor of 30, thereby significantly affecting the equilibrium binding affinities. While this large difference at first seems remarkable, it can be explained by sequence effects as described below.

A six-ring hairpin PA without a β substitution, KA1039, was also tested to evaluate the effects of the number of ring systems on the equilibrium binding and kinetics with the same cognate DNA. As expected, the binding affinity of KA1039 was weaker, and the data show that it decreased by a factor of 25 relative to that of KA1002 with eight rings. The reduction of the number of rings significantly decreased the association rate of KA1039 relative to that of KA1002, whereas an only 2-fold increase in the dissociation rate was observed. It is appealing that the six-ring compound actually binds more strongly than the eight-ring KA1007. All of the experiments have been repeated at least three times, and the results are quite reproducible. The experimental errors in Table 1 are based on the repeat variations.

ITC of the Thermodynamics of Polyamide–DNA Interactions. While the large ΔG for polyamide binding can be obtained most accurately from SPR, a more detailed energetic understanding of the interactions requires direct enthalpy determination by ITC.^{24,25} Because of the experimental limitations for the large K values for the binding of PAs to TGGCTT, only the binding enthalpies, ΔH , could be obtained at the concentrations required in ITC experiments. ΔH was determined at low molar ratios of compounds to DNA because of potential strong aggregation of the hairpin PAs at high concentrations and molar ratios to DNA. In this type of experiment, all added compound is bound to DNA and the binding ΔH can be directly determined from the average binding heat per mole without any specific fitting model by simply subtracting the integrated peak areas for ligand/buffer titration from the ligand/DNA titration.^{26,27} Several concentrations of the PA and DNA were used to test for possible aggregation effects of the PA in ITC titrations. Figure 3 shows a titration of KA1039 into TGGCTT with the buffer blank correction, and the ΔH value for binding is -11.1 ± 0.5 kcal/mol at 25 °C. The ΔH values for the titration at concentrations from 25 to 50 μM were similar (not shown) and suggest that with this PA, aggregation is not a problem under ITC conditions. ITC experiments for the larger eight-ring or β -containing PAs were tried at several concentrations without success. Increasing the temperature of the ITC experiment to 45 °C still did not allow consistent determination of ΔH of the large PAs. On the basis of the erratic and noisy titration curves obtained, this is probably due to aggregation of the longer PAs at ITC concentrations.²⁸

The heat capacity (ΔC_p) of KA1039 has been determined by conducting the ITC titrations at different temperatures. The

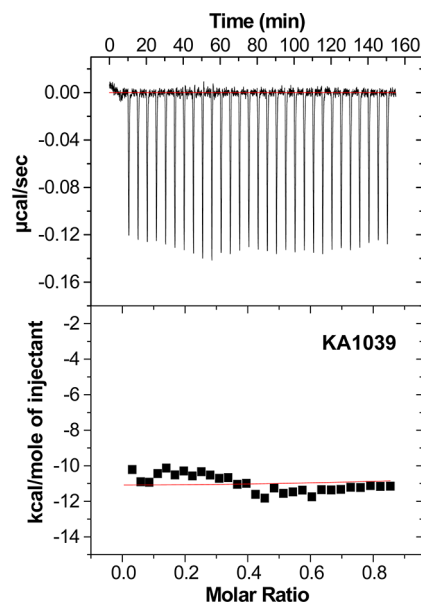


Figure 3. ITC titration of 37.5 μM KA1039 into 10 μM TGGCTT hairpin duplex at 25 °C (top). Integrated heats after subtraction of the heat of dilution plotted vs KA1039:DNA molar ratio (bottom).

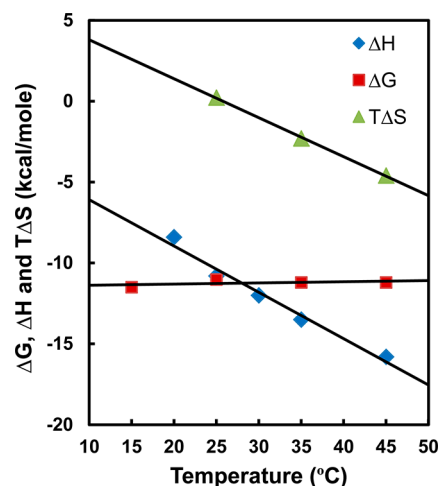


Figure 4. Thermodynamic results, ΔG from SPR, ΔH from ITC, and $T\Delta S$ calculated from $\Delta G = \Delta H - T\Delta S$, for binding of KA1039 to the TGGCTT site at different temperatures.

profile of ΔH versus temperature is shown in Figure 4, and a linear fit yields a ΔC_p of $-287 \text{ cal M}^{-1} \text{ K}^{-1}$. On the basis of SPR binding free energy values, $\Delta G = -RT \ln K$, and the ITC enthalpy values, the $T\Delta S$ values were calculated from $\Delta G = \Delta H - T\Delta S$ at different temperatures (Figure 4). Comparison of the contributions of the enthalpy and entropy to the free energy shows that PA complex formation is dominated by the favorable binding enthalpy.

Evaluation of Binding Mode and DNA Structural Changes by CD. Binding of PAs to the TGGCTT site as a function of compound concentration is evaluated by CD spectroscopy. The CD signals monitor the asymmetric environment of the compounds when they are bound to DNA and thus can be used to obtain information about the binding mode.²⁹ In Figure 5, the CD results for the hairpin PA complexes are characterized by large, positive induced signals from 300 to 400 nm, where the compounds absorb and the DNA signals do not

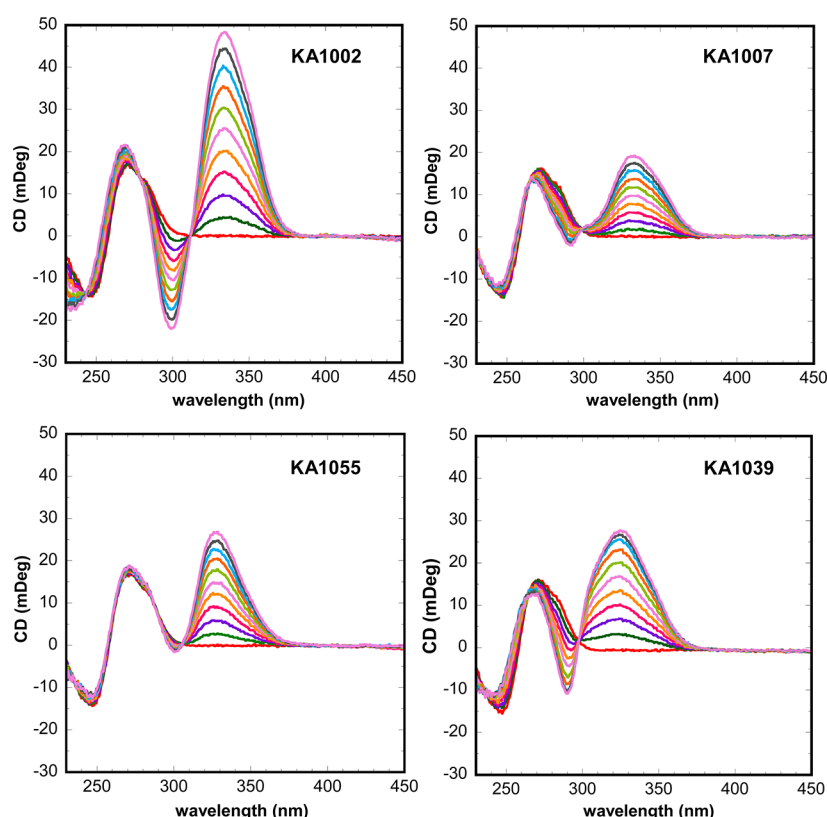


Figure 5. Induced CD signals for TGGCTT with all PAs in HEPES buffer at 25 °C. Molar ratios of compound to DNA hairpin are from 0 to 2.0 as the induced CD signal for the PAs increases.

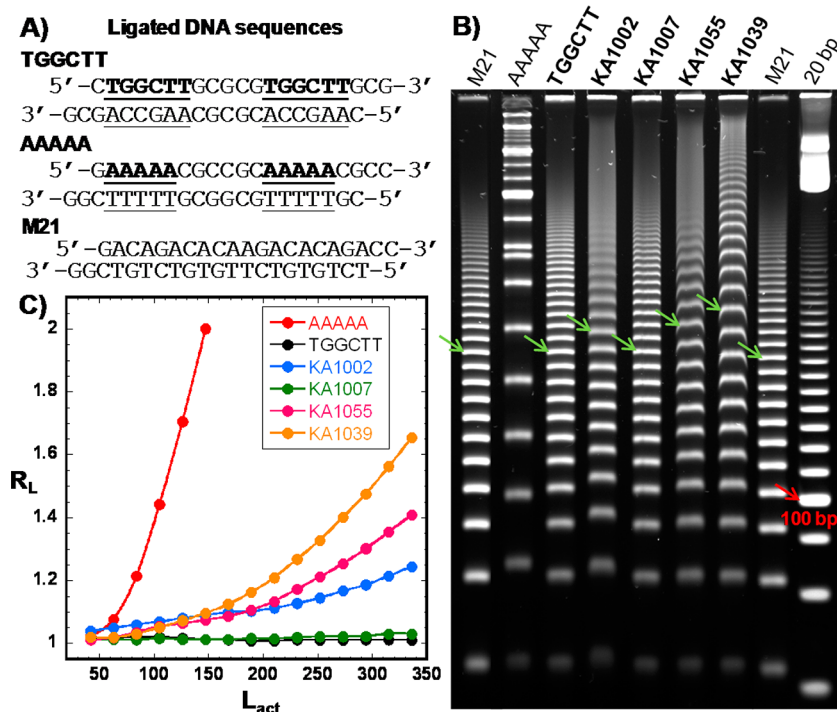


Figure 6. (A) Ligation ladder sequence of TGGCTT, AAAAA, and M21. (B) Eight percent (29:1) native polyacrylamide gel of TGGCTT with four PAs. All PAs were incubated with the TGGCTT duplex in a 4:1 ligand:binding site molar ratio. A 21 bp marker (M21) and a 20 bp marker are loaded as the migration standards, and AAAAA is shown as the curvature standard. Arrows indicate the 252 bp ligated multimers. (C) Plot of the relative mobility, R_L , as a function of L_{act} for AAAAA and TGGCTT in the absence and presence of the PAs.

interfere. The large positive induced CD signals indicate a minor groove mode of binding as expected for these PAs.³⁰ All the

titrations were conducted incrementally from a 0:1 to 2:1 molar ratio of ligand to binding site. The strongest binder among four

ligands, KA1002, induced the largest CD signals upon binding followed by KA1055, KA1039, and the weaker binder, KA1007. Moreover, negative induced signals have been observed with KA1002 and KA1039 around 300 nm where they absorb, but not with β -containing KA1007 and KA1055. This observation could be simply due to the loss of one heterocyclic unit in the β derivatives and/or the fact that the introduction of β changes the environment of the PA–DNA minor groove complex. There is not a large change in the DNA CD signals upon binding of any of the compounds, suggesting that they do not cause major changes in DNA base stacking.

Mobility and Curvature Changes Induced by Polyamide Binding Assessed by Gel Electrophoresis. Ladders of ligated DNA sequences, which have phased binding sequences (Figure 6A), provide an excellent method for evaluating binding-induced structural changes in different sequences.^{31,32} The method provides information about structure and binding-induced effects that complements the results from CD, such as the DNA bending angles that cannot be obtained through CD. PAGE results for ligation ladders of the TGGCTT sequence without and with PAs are compared in Figure 6B. The molecular weight of each gel band was assigned by adding 21 bp to each sequential band starting from the one with the highest mobility and using both the M21 and 20 bp ligation markers for additional reference. In Figure 6B, as indicated by the arrows, the 252 bp ligated multimers were used to compare the DNA mobility. This DNA size was used for comparison because its mobility changes are more prominent than the shorter ladders and it is well separated from other ligated multimers. The gel results show that the unbound TGGCTT migrated at approximately the same rate as the random sequence, mobility marker, M21, which indicates that TGGCTT is relatively straight. Mobility retardation of TGGCTT is observed upon addition of KA1002, KA1055, and KA1039, but not KA1007. Among all the ligands, KA1039, the compound containing six heterocyclic rings, decreased the target sequence's mobility the most.

The relative mobility (R_L), where $R_L = L_{\text{apparent}}/L_{\text{actual}}$, was calculated for each ligation ladder and plotted as a function of L_{actual} for each sample (Figure 6C). L_{actual} is the actual molecular weight in base pairs of each ligated multimer, and L_{apparent} is the apparent molecular weight in base pairs determined according to the distance, relative to the standard, each ladder migrates in the gel. The R_L values of marker M21 have been normalized to 1.0, and thus, an R_L value of >1.0 indicates lower mobility, which suggests a more curved DNA structure.³³ From the R_L values, it is obvious that the R_L value of unbound TGGCTT is slightly greater than 1, and the enhancement of R_L values is the most significant with the binding of KA1039, followed by KA1055 and KA1002. KA1007 increased the R_L values very slightly, and the change is not detectable until the multimers are longer than 210 bp. The retarded mobilities and increasing R_L values suggest that the relatively straight TGGCTT sequence has been bent upon binding of the PAs.

To quantitatively evaluate the effects of PA on DNA curvature, a well-studied sequence, AAAAA [A5 (Figure 6A)], was used as a reference. The phased A5-containing sequences migrate much slower than their true molecular weight in the gel (Figure 6B) because A5 tracts bend the DNA structure by 18° per helical turn.^{31,34} The PA curvature calculations are as described previously.^{31,33,34} Briefly, R_L values for ligated multimers in range of 105 bp $\leq L_{\text{actual}} \leq$ 189 bp were averaged over three gel experiments for A5. Data were fit to the equation $R_L - 1 = (aL_{\text{actual}}^2 - b)C_r^2$, where C_r is the relative curvature and equals 1.0

for AAAAA by definition. From the linear fit, values for a and b were determined giving $R_L - 1 = (-0.086 + 4.943 \times 10^{-5}L_{\text{actual}}^2)C_r^2$. Using this equation, the relative curvature, C_r values, for unbound TGGCTT and the complexes can be determined (Table 3). The C_r values can be converted to bending angles with

Table 3. Relative Curvatures (C_r) and Calculated Bend Angles (θ) for Free DNAs and Hairpin PA Complexes

	C_r^a	θ (deg)
AAAAA	1.00	18
TGGCTT	≈ 0	0
KA1002	0.165	3.0
KA1007	≈ 0	0
KA1055	0.203	3.7
KA1039	0.302	5.4

^aThe error in C_r is less than ± 0.025 .

a C_r value of 1.0 being equivalent to an 18° bending. Free TGGCTT is a straight sequence ($C_r \approx 0$), while the binding of KA1002, KA1055, and KA1039 bent TGGCTT by 3°, 3.7°, and 5.4° per helical turn, respectively. The bending angle for KA1007 is essentially zero.

DISCUSSION

PAs have reached a level of development where they can effectively compete with transcription factors in terms of both affinity and sequence specificity.^{3,5,35} Part of their development has been the replacement of one or more of the pyrrole or imidazole heterocycles with flexible β . This substitution can allow improved conformational adjustment and matching of PAs to the local DNA minor groove shape. Dervan, Sugiyama, and others have shown the advantages of replacing a heterocycle with a β in terms of improved affinity, particularly as the number of heterocycles in the PAs is increased.^{8,14,16} There have, however, been relatively few published studies of effects of substitution of a single heterocycle with a β . Preliminary studies¹⁷ suggested that a single β could cause a significant decrease in the affinity of sequences targeted to an Ets transcription factor binding site. With other sequence contexts, a single β substitution can increase the affinity of PA for its cognate site.¹⁴ To obtain additional information about the molecular basis for the unexpected decrease in affinity, a Py residue was substituted with β in the same PA but on the C-terminal side of the γ hairpin loop (Figure 1); the original analysis was conducted with a β on the N-terminal side. More detailed studies of both β -substituted compounds as well as the unsubstituted parent PA have been conducted with additional DNA sequences, including both thermodynamic and structural methods.

Effects of PA and DNA Sequence on Relative Binding Affinity. It is important that the influence of a β on the PA binding varies significantly with position (KA1055 vs KA1007). To improve our understanding of the positional effects of β substitution, five mutant DNA sequences have been studied with KA1002 and KA1055 (Table 2). KA1002 binds more strongly to the mutant 1 sequence, 5'-TGCCTT-3', than to the cognate. Although this seems striking, the switch of the middle G/C base pair into C/G base pair actually can reverse the binding orientation of KA1002. The original orientation is N \rightarrow C (ImImPyPy) of KA1002 bound 5' \rightarrow 3' to 5'-TTGGCTT-3', while with the mutant 1 sequence, it becomes N \rightarrow C (ImImPyPy) targeting 5' \rightarrow 3' to 5'-AAGCCAA-3'. The stacked Py/Py near the γ loop might be targeting the A·T base pair more

strongly in the mutant than the T·A base pair in the original sequences to give a greater ΔT_m value. For mutant sequences 2–5, ΔT_m values are smaller than for the cognate site as expected. Through the comparison of ΔT_m values for mutants 2–4 and their substitution positions, it is clear that mutation of the fourth base pair of the 5′-TGGCTT-3′ site (mutant 3, 5′-TGGGTT-3′) decreases the thermal stability much more significantly than mutation of the fifth base pair (mutant 4, 5′-TGGCCT-3′), while the mutant at the third base pair (mutant 2, 5′-TGTCTT-3′) influences the binding the least. Once both the third and fourth base pairs have been mutated, mutant 5 (5′-TGATTTT-3′), there is only a weak interaction between KA1002 and DNA as indicated by the very slight increase in ΔT_m . The ΔT_m values for KA1055 show that this β substitution containing PA also prefers mutant 1, 5′-TGCCTT-3′, more than the cognate sequence, TGGCTT, but the increase is smaller than that for KA1002. The ΔT_m values with mutant sequences 3 and 5 are similar but weaker than for the cognate site. This indicates that in some cases β substitution not only can weaken the PA's binding affinity but also can reduce the selectivity of DNA recognition on both binding and flanking sites. Moreover, the ΔT_m values clearly show that the mutation of the fourth base pair reduces the binding affinity more than the mutations of the third and fifth base pairs as observed with KA1002 binding. The PA position-dependent effects on DNA interactions are in agreement with the mutation results and provide new insight into PA–DNA interaction affinity. KA1055, which has the β targeting the least sensitive third base pair of TGGCTT, displays a binding affinity comparable to that of KA1002, while KA1007, which has the β targeting the most sensitive fourth base pair of TGGCTT, shows much weaker binding than KA1002. In summary, the different contributions of the base pairs in the targeting site cause distinct affinity reductions for the β -substituted PA and different effects on binding affinities for the PA-bound DNA mutants.

SPR Binding Affinity and Kinetics. In an effort to improve our understanding of the energetic effects of incorporating a β into PA on DNA recognition, comprehensive kinetic studies were conducted with biosensor surface plasmon resonance techniques. SPR results show that the PAs exhibit a wide range of equilibrium binding affinities with significant differences in their association and dissociation rates (Table 1). The unsubstituted parent eight-ring PA, KA1002, has the highest affinity, and its association rates suggest a well-optimized shape for the minor groove. The very slow dissociation rates and large negative ΔH for binding indicate very efficient H-bond indexing with the cognate DNA sequence and a large energetic penalty required to break all the favorable interactions to release the compound from the groove. PAs, such as KA1002, have a number of conformations in solution because of single-bond rotational possibilities about the amide bonds. They must, however, adopt only the single conformation with an appropriate crescent shape to match the minor groove structure in the DNA complex. In addition, they form numerous interactions with DNA that must be appropriately aligned in the complex. The rearrangement and alignment slow the association reaction, but once formed, the complex can be exceptionally stable, as with KA1002, with a very slow dissociation reaction. The two β -substituted PAs, KA1007 and KA1055, have much slower association rates than KA1002. This can be explained by the increased flexibility of the β group and the increased number of conformations in solution that do not have a shape to match the DNA minor groove. Binding DNA requires more time than that for PAs with only heterocycles and will slow the kinetics of association.

The association rates for β -substituted KA1007 and KA1055 are very similar, but there is a significant difference in the first-order dissociation rates. The N-terminal side β -substituted KA1007 exhibits a faster dissociation rate, whereas C-terminal β -substituted KA1055 has a slower dissociation rate than KA1002. The position of the β on affinity that was noted in the ΔT_m results also has a strong effect on the dissociation rates. This is the first instance in which the position of the β was also shown to have such a large effect on dissociation rates and affinities of PAs in the same binding site.

KA1039 is a six-heterocycle PA that is very similar to the eight-ring KA1002 but binds to a shorter sequence in the same DNA site. The reduction in the number of heterocycles in KA1039 not only decreases the binding affinity, as expected because of the decrease in the number of potential H-bonding moieties, but also decreases the association rate of KA1039 as the slowest among all four PAs. This result suggests that the smaller PA has a larger number of nonspecific binding orientations that effectively reduce its available concentration for binding and result in a slower association rate. Once bound, however, KA1039 forms strong H-bonds with a large negative ΔH for binding to the cognate DNA site and dissociates more slowly than KA1007. KA1039 has the same critical N-terminal Im-Im-Py sequence as the strong binders KA1002 and KA1055, and this accounts for its dissociation being slower and its binding stronger than those of KA1007.

All PAs in this study have relatively high molecular weights and very high binding constants but only a single charge (Figure 1). Therefore, the effect of electrostatic contributions upon binding of PAs to DNA and the effects of salt concentrations on binding affinity are expected to be small under the experimental conditions used in this study.

Binding Thermodynamics. ITC experiments were not successful at the required concentrations ($>5 \mu\text{M}$) for the larger PAs, presumably because of aggregation,²⁸ but have been conducted successfully for the six-ring KA1039. To the best of our knowledge, there are no reports of calorimetric studies for eight-ring PAs in the literature, probably also because of aggregation effects at ITC concentrations. Breslauer and co-workers observed ITC results comparable to those of KA1039 for a different six-ring polyamide, ImImPy- γ -PyPyPy- β -Dp,³⁶ and although additional studies are needed, the similarity of the two results suggests that a large negative enthalpy is a common feature of PA–DNA complexes. For the eight-ring KA1002 and its β -substituted analogue KA1055, the SPR free energies are higher than for KA1039, which suggests that their binding affinities are also quite enthalpy-dependent.

The full thermodynamic data for binding of KA1039 to the TGGCTT site are summarized in Figure 4. The SPR Gibbs free energy of formation of the KA1039–DNA complex changes very little at temperatures from 15 to 45 °C, while the binding-induced enthalpy becomes remarkably more negative, more favorable for complex formation, as the temperature is increased. The calculated $T\Delta S$ values also become more negative, less favorable for complex formation. Figure 4 shows that the binding of KA1039 is strongly enthalpy-driven below 25 °C and becomes entirely enthalpy-driven above 25 °C. A large and negative ΔC_p for KA1039 binding ($-287 \text{ cal M}^{-1} \text{ K}^{-1}$) has been calculated from the slope of ΔH versus temperature. The favorable enthalpy and unfavorable entropy terms suggest that the interaction of KA1039 and DNA is largely driven by the H-bonding between them, and little high-entropy water, as is observed in the narrow A-tract minor grooves, has been released because of the relatively

wide minor groove in TGGCTT. The thermodynamic profile is characteristic of biomolecular processes, such as protein folding, that are stabilized by numerous relative weak individual interactions that sum to a quite favorable net ΔG .

Minor Groove Geometry and Overall DNA Structure.

Gel electrophoresis with ligation ladder assays is a well-established, sensitive method for evaluating the DNA overall curvature and the minor groove geometry through changes in DNA mobility. An A-tract (Figure 6A) narrows the minor groove and induces an intrinsically curved overall structure that displays anomalously slow mobilities in ligation ladder PAGE.^{31,34} Results with TGGCTT indicate that the overall structure is essentially straight and the minor groove of the TGGCTT site is relatively wide. This observation is consistent with previous studies that showed that the minor groove is widened by the introduction of G·C base pairs.³⁷

A relatively small amount of DNA bending has been observed by the binding of KA1002, KA1055, and KA1039 to the cognate DNA (Table 2). This bending can be either toward the major groove or toward the minor groove depending on the changes in the local geometry of the minor groove. In the literature, the dimer formation of a natural PA, distamycin, at an alternating AT site widens the minor groove and changes the DNA bending directionality from minor groove to major groove with a 15–20° curvature.³⁸ Dervan and Chenoweth have shown that cyclic eight-ring PAs also widen the minor groove and compress the major groove with bending toward the major groove by around 20° upon minor groove targeting [Protein Data Bank entry 3OMJ (Figure S12A of the Supporting Information)].^{39,40} It seems likely, therefore, that the hairpin PA binding-induced bending in this study should be the consequence of an expanded minor groove with bending toward the major groove. The small bending angles indicate a relatively small change in the overall DNA structure as in ref 41 (Figure S12B of the Supporting Information),⁴¹ and this evaluation agrees with the small DNA spectral changes in CD spectra with PA complexes (Figure 5).

Through the comparison of the gel mobility and binding-induced DNA bending angle for each polyamide complex, it is clear that the substitution of Py with β can influence the minor groove geometry in addition to its strong effect on the binding affinity and kinetics. The β -substituted molecule KA1055 bends DNA slightly more than the parent KA1002, while KA1007, the other β -substituted PA studied here, bends DNA less. This result suggests a poor minor groove interaction of KA1007 without a significant effect on the DNA conformation. KA1055, however, which has β adjacent to a different, more important DNA base position, has a significant effect on DNA structure. Interestingly, the binding of the six-ring PA, KA1039, affects the minor groove structure more than the larger PAs, resulting in the most curved DNA conformation described here. A possible cause of this large effect is that the six-ring PA has a better fit to the DNA minor groove shape and is able to optimize affinity by inducing a larger conformational change in DNA. As PAs increase in size, they become too curved and rigid to match and alter the DNA minor groove shape,^{42,43} and this may account for the effects of the six-ring system. The structural effects of the number of heterocycles, however, need to be investigated in more detail with additional PAs. The observed binding-induced DNA conformational changes might allow KA1002, KA1055, and KA1039 to perform as allosteric modulators of DNA transcription in terms of compressing the major groove and reducing the binding affinity of major groove targeting transcription factors. Studies that aim to evaluate this possibility are in progress.

In summary, the energetic and structural effects of positional substitution of Py with a β and a reduction in the number of heterocycles on hairpin PA–DNA binding have been investigated in detail. Reduced binding affinity has been observed for all the modified PAs, KA1007, KA1055, and KA1039, relative to that of KA1002. It is very exciting, however, that the effects of DNA mutation on binding of a single PA as well as the effects of the position of β substitution on binding tell a very important story about PA–DNA complexes. It is clear that the heterocycles and β interact very differently with DNA bases in a minor groove, position-dependent manner. Comparison of mutant DNA sequences with KA1002 and KA1055 also shows a significantly different effect in recognition of T·A versus A·T base pairs. Clearly, these differences need to be investigated further with other PA sequences and DNAs, and such studies are underway.

■ ASSOCIATED CONTENT

Supporting Information

Supporting figures (Figures S1–S12). This material is available free of charge via the Internet at <http://pubs.acs.org>.

■ AUTHOR INFORMATION

Corresponding Author

*W.D.W.: telephone, (404) 413-5503; fax, (404) 413-5505; e-mail, wdw@gsu.edu. J.K.B.: telephone, (314) 516-7352; fax, (314) 516-5342; e-mail, bashkinj@umsl.edu.

Funding

This work was supported by National Institute of Allergy and Infectious Diseases (NIAID) Grant AI064200 to W.D.W., NIAID Grant AI083803 to J.K.B., financial support from NanoVir, LLC (to J.K.B.), and a Georgia State University Molecular Basis of Disease Fellowship (to S.W.).

Notes

J.K.B. declares that he is part owner of NanoVir, LLC.

■ ACKNOWLEDGMENTS

We thank the Danforth Plant Science Center for HRMS [National Science Foundation (NSF) Grant DBI 0922879]. We thank the NSF for a grant (CHE-0959360) to purchase the 600 MHz NMR instrument used in this work.

■ ABBREVIATIONS

PA, polyamide; T_m , thermal melting; SPR, biosensor surface plasmon resonance; ITC, isothermal titration calorimetry; CD, circular dichroism; PAGE, polyacrylamide gel electrophoresis; β , β -alanine.

■ REFERENCES

- (1) Dervan, P. B. (2001) Molecular recognition of DNA by small molecules. *Bioorg. Med. Chem.* 9, 2215–2235.
- (2) Bando, T., and Sugiyama, H. (2006) Synthesis and biological properties of sequence-specific DNA-alkylating pyrrole-imidazole polyamides. *Acc. Chem. Res.* 39, 935–944.
- (3) Suckling, C. J. (2008) Molecular recognition and physicochemical properties in the discovery of selective antibacterial minor groove binders. *J. Phys. Org. Chem.* 21, 575–583.
- (4) Lacy, E. R., Madsen, E. M., Lee, M., and Wilson, W. D. (2003) Polyamide dimer stacking in the DNA minor groove and recognition of TG mismatched base pairs in DNA. In *DNA and RNA Binders, From Small Molecules to Drugs* (Demeunynck, M., Bailly, C., and Wilson, W. D., Eds.) Vol. 1, pp 384–413, Wiley-VCH Verlag GmbH & Co. KGaA, Weinheim, Germany.

- (5) Moretti, R., Donato, L. J., Brezinski, M. L., Stafford, R. L., Hoff, H., Thorson, J. S., Dervan, P. B., and Ansari, A. Z. (2008) Targeted chemical wedges reveal the role of allosteric DNA modulation in protein–DNA assembly. *ACS Chem. Biol.* 3, 220–229.
- (6) Chaires, J. B. (2008) Allostery: DNA does it, too. *ACS Chem. Biol.* 3, 207–209.
- (7) Matsuda, H., Fukuda, N., Ueno, T., Katakawa, M., Wang, X., Watanabe, T., Matsui, S., Aoyama, T., Saito, K., Bando, T., Matsumoto, Y., Nagase, H., Matsumoto, K., and Sugiyama, H. (2011) Transcriptional inhibition of progressive renal disease by gene silencing pyrrole-imidazole polyamide targeting of the transforming growth factor- β 1 promoter. *Kidney Int.* 79, 46–56.
- (8) Edwards, T. G., Koeller, K. J., Slomczynska, U., Fok, K., Helmus, M., Bashkin, J. K., and Fisher, C. (2011) HPV episome levels are potentially decreased by pyrrole-imidazole polyamides. *Antiviral Res.* 91, 177–186.
- (9) Franks, A., Tronrud, C., Kiakos, K., Kluza, J., Munde, M., Brown, T., Mackay, H., Wilson, W. D., Hochhauser, D., Hartley, J. A., and Lee, M. (2010) Targeting the ICB2 site of the topoisomerase II α promoter with a formamido-pyrrole-imidazole-pyrrole H-pin polyamide. *Bioorg. Med. Chem.* 18, 5553–5561.
- (10) Raskatov, J. A., Meier, J. L., Puckett, J. W., Yang, F., Ramakrishnan, P., and Dervan, P. B. (2012) Modulation of NF- κ B-dependent gene transcription using programmable DNA minor groove binders. *Proc. Natl. Acad. Sci. U.S.A.* 109, 1023–1028.
- (11) Wang, X., Nagase, H., Watanabe, T., Nobusue, H., Suzuki, T., Asami, Y., Shinojima, Y., Kawashima, H., Takagi, K., Mishra, R., Igarashi, J., Kimura, M., Takayama, T., Fukuda, N., and Sugiyama, H. (2010) Inhibition of MMP-9 transcription and suppression of tumor metastasis by pyrrole-imidazole polyamide. *Cancer Sci.* 101, 759–766.
- (12) Raskatov, J. A., Hargrove, A. E., So, A. Y., and Dervan, P. B. (2012) Pharmacokinetics of Py-Im polyamides depend on architecture: Cyclic versus linear. *J. Am. Chem. Soc.* 134, 7995–7999.
- (13) Kamei, T., Aoyama, T., Tanaka, C., Nagashima, T., Aoyama, Y., Hayashi, H., Nagase, H., Ueno, T., Fukuda, N., and Matsumoto, Y. (2012) Quantitation of pyrrole-imidazole polyamide in rat plasma by high-performance liquid chromatography coupled with UV detection. *J. Biomed. Biotechnol.*, DOI: 10.1016/j.biotech.2012.09.023.
- (14) Wang, C. C. C., Ellervik, U., and Dervan, P. B. (2001) Expanding the recognition of the minor groove of DNA by incorporation of β -alanine in hairpin polyamides. *Bioorg. Med. Chem.* 9, 653–657.
- (15) Urbach, A. R., Love, J. J., Ross, S. A., and Dervan, P. B. (2002) Structure of a β -alanine-linked polyamide bound to a full helical turn of purine tract DNA in the 1:1 motif. *J. Mol. Biol.* 320, 55–71.
- (16) Fukuda, N., Ueno, T., Tahira, Y., Ayame, H., Zhang, W., Bando, T., Sugiyama, H., Saito, S., Matsumoto, K., Mugishima, H., and Serie, K. (2006) Development of gene silencing pyrrole-imidazole polyamide targeting the TGF- β 1 promoter for treatment of progressive renal diseases. *J. Am. Soc. Nephrol.* 17, 422–432.
- (17) Bashkin, J. K., Aston, K., Ramos, J. P., Koeller, K. J., Nanjunda, R., He, G., Dupureur, C. M., and Wilson, W. D. (2012) Promoter scanning of the human COX-2 gene with 8-ring polyamides: Unexpected weakening of polyamide-DNA binding and selectivity by replacing an internal N-Me-pyrrole with β -alanine. *Biochimie.*
- (18) Dupureur, C. M., Bashkin, J. K., Aston, K., Koeller, K. J., Gaston, K. R., and He, G. (2012) Fluorescence assay of polyamide-DNA interactions. *Anal. Biochem.* 423, 178–183.
- (19) Nanjunda, R., Munde, M., Liu, Y., and Wilson, W. D. (2011) Real-time monitoring of nucleic acid interactions with biosensor-surface plasmon resonance. In *Methods for Studying Nucleic Acid/Drug Interactions* (Wanunu, M., and Tor, Y., Eds.) pp 91–122, CRC Press, Boca Raton, FL.
- (20) Davis, T. M., and Wilson, W. D. (2000) Determination of the refractive index increments of small molecules for correction of surface plasmon resonance data. *Anal. Biochem.* 284, 348–353.
- (21) Morton, T. A., and Myszkowski, D. G. (1998) Kinetic analysis of macromolecular interactions using surface plasmon resonance biosensors. *Methods Enzymol.* 295, 268–294.
- (22) Karlsson, R. (1999) Affinity analysis of non-steady-state data obtained under mass transport limited conditions using BIAcore technology. *J. Mol. Recognit.* 12, 285–292.
- (23) Wilson, W. D., Tanious, T. A., Fernandez-Saiz, M., and Rigl, C. T. (1997) Evaluation of drug-nucleic acid interactions by thermal melting curves. *Methods Mol. Biol.* 90, 219–240.
- (24) Mazur, S., Tanious, F. A., Ding, D., Kumar, A., Boykin, D. W., Simpson, I. J., Neidle, S., and Wilson, W. D. (2000) A thermodynamic and structural analysis of DNA minor-groove complex formation. *J. Mol. Biol.* 300, 321–337.
- (25) Wang, L., Kumar, A., Boykin, D. W., Bailly, C., and Wilson, W. D. (2002) Comparative thermodynamics for monomer and dimer sequence-dependent binding of a heterocyclic dication in the DNA minor groove. *J. Mol. Biol.* 317, 361–374.
- (26) Ren, J. S., Jenkins, T. C., and Chaires, J. B. (2000) Energetics of DNA intercalation reactions. *Biochemistry* 39, 8439–8447.
- (27) Liu, Y., Kumar, A., Depauw, S., Nhili, R., David-Cordonnier, M. H., Lee, M. P., Ismail, M. A., Farahat, A. A., Say, M., Chackal-Catoen, S., Batista-Parra, A., Neidle, S., Boykin, D. W., and Wilson, W. D. (2011) Water-mediated binding of agents that target the DNA minor groove. *J. Am. Chem. Soc.* 133, 10171–10183.
- (28) Hargrove, A. E., Raskatov, J. A., Meier, J. L., Montgomery, D. C., and Dervan, P. B. (2012) Characterization and solubilization of pyrrole-imidazole polyamide aggregates. *J. Med. Chem.* 55, 5425–5432.
- (29) Rodger, A., and Norden, B. (1997) *Circular Dichroism and Linear Dichroism*, Oxford University Press, New York.
- (30) Lyng, R., Rodger, A., and Norden, B. (1992) The CD of ligand-DNA systems. 2. Poly(dA-dT) B-DNA. *Biopolymers* 32, 1201–1214.
- (31) Tevis, D. S., Kumar, A., Stephens, C. E., Boykin, D. W., and Wilson, W. D. (2009) Large, sequence-dependent effects on DNA conformation by minor groove binding compounds. *Nucleic Acids Res.* 37, 5550–5558.
- (32) Hunt, R. A., Munde, M., Kumar, A., Ismail, M. A., Farahat, A. A., Arafa, R. K., Say, M., Batista-Parra, A., Tevis, D., Boykin, D. W., and Wilson, W. D. (2011) Induced topological changes in DNA complexes: Influence of DNA sequences and small molecule structures. *Nucleic Acids Res.* 39, 4265–4274.
- (33) Ross, E. D., Den, R. B., Hardwidge, P. R., and Maher, L. J. (1999) Improved quantitation of DNA curvature using ligation ladders. *Nucleic Acids Res.* 27, 4135–4142.
- (34) Crothers, D. M., and Drak, J. (1992) Global features of DNA-structure by comparative gel-electrophoresis. *Methods Enzymol.* 212, 46–71.
- (35) Oyoshi, T., Kawakami, W., Narita, A., Bando, T., and Sugiyama, H. (2003) Inhibition of transcription at a coding sequence by alkylating polyamide. *J. Am. Chem. Soc.* 125, 4752–4754.
- (36) Pilch, D. S., Poklar, N., Baird, E. E., Dervan, P. B., and Breslauer, K. J. (1999) The thermodynamics of polyamide-DNA recognition: Hairpin polyamide binding in the minor groove of duplex DNA. *Biochemistry* 38, 2143–2151.
- (37) Wemmer, D. E., Geierstanger, B. H., Fagan, P. A., Dwyer, T. J., Jacobsen, J. P., Pelton, J. G., Ball, G. E., Leheny, A. R., Chang, W.-H., Bathini, Y., Lown, J. W., Rentzeperis, D., Marky, L. A., Singh, S., and Kollman, P. (1994) Minor groove recognition of DNA by distamycin and its analogs. In *Structural Biology: The state of the art* (Sarma, R. H., and Sarma, M. H., Eds.) Vol. 2, pp 301–323, Adenine Press, Schenectady, NY.
- (38) Wang, S., Munde, M., Wang, S., and Wilson, W. D. (2011) Minor groove to major groove, an unusual DNA sequence-dependent change in bend directionality by a distamycin dimer. *Biochemistry* 50, 7674–7683.
- (39) Chenoweth, D. M., and Dervan, P. B. (2010) Structural basis for cyclic Py-Im polyamide allosteric inhibition of nuclear receptor binding. *J. Am. Chem. Soc.* 132, 14521–14529.
- (40) Chenoweth, D. M., and Dervan, P. B. (2009) Allosteric modulation of DNA by small molecules. *Proc. Natl. Acad. Sci. U.S.A.* 106, 13175–13179.
- (41) Wang, Y., Ma, N., Wang, Y., and Chen, G. (2012) Allosteric analysis of glucocorticoid receptor-DNA interface induced by cyclic Py-

Im polyamide: A molecular dynamics simulation study. *PLoS One* 7, e35159.

(42) Kelly, J. J., Baird, E. E., and Dervan, P. B. (1996) Binding site size limit of the 2:1 pyrrole-imidazole polyamide-DNA motif. *Proc. Natl. Acad. Sci. U.S.A.* 93, 6981–6985.

(43) Turner, J. M., Swalley, S. E., Baird, E. E., and Dervan, P. B. (1998) Aliphatic/aromatic amino acid pairings for polyamide recognition in the minor groove of DNA. *J. Am. Chem. Soc.* 120, 6219–6226.